

1 **Impacts of spatial uncertainty on performance of age structure-**
2 **based harvest strategies**

3 Gavin Fay^{a,b}, André E. Punt^b, and Anthony D.M. Smith^a

4

5 ^a CSIRO Marine and Atmospheric Research, Castray Esplanade, Hobart TAS 7001,
6 Australia.

7 ^b School of Aquatic and Fishery Sciences, University of Washington, Seattle WA
8 98195-5020, USA.

9

10 Corresponding author: Gavin Fay

11 Phone: +61-3-6232-5321

12 Fax: +61-3-6232-5000

13 Email: gavin.fay_at_csiro.au

14

DRAFT

15 **1. Abstract**

16 Harvest Control Rules (HCRs), key components of fisheries management strategies, are used to
17 calculate recommended catch levels given estimates of present stock status or levels of fishing
18 mortality. The performance of HCRs when confronted with spatial variability, either from
19 population dynamics, fishery operations, or in data collection, are poorly understood. Australia's
20 Southern and Eastern scalefish and shark fishery (SESSF) uses a tier framework of HCRs, with
21 the choice of which Tier rule to apply for a species reflecting the uncertainty in available
22 information on stock status.

23 A Management Strategy Evaluation (MSE) approach is used to evaluate the performance of a
24 'data-poor' (Tier 3) HCR, which uses information from the age structure of the catch only, when
25 applied to the fishery for blue eye trevalla (*Hyperoglyphe antarctica*): a long-lived, late-
26 maturing species exhibiting spatial variability, potentially a result of structure in the population
27 dynamics. Several versions of the Tier 3 HCR are tested, varying in the types of reference points
28 used to determine management actions, and in the way spatial variability is accounted for when
29 setting catch limits.

30 Results suggest effective implementation of the HCRs is challenging, and requires appropriate
31 choice of reference points and estimators. Spatial disaggregation of data leads to uncertain
32 estimates of current mortality. However, appropriate weighting of spatial estimates of stock
33 status leads to improved conservation of the resource over 'pooled data' approaches. Variability
34 in performance measures are dominated by uncertainties regarding whether the assumed value
35 for the rate of natural mortality, M is correct or not, and the true value for the steepness of the
36 stock-recruitment relationship. Indeed, simulated outcomes are sensitive to many uncertainties
37 inherent to an information-poor, spatially-heterogeneous resource. Additional considerations
38 besides the HCR should be taken to achieve a desired precautionary result in contrast to the
39 situation for more data-rich scenarios.

40 **2. Introduction**

41 Harvest strategies (often termed Management Procedures) are well recognized as effective tools
42 for conservation of natural resources and have been applied widely in fisheries management,
43 principally in output control, data-rich fisheries (*e.g.* Butterworth et al. 1997, Butterworth and
44 Punt 1999, Cooke 1999, Kell et al. 1999, 2005). Harvest strategies consist of the following
45 components: data collection schemes, assessment methods, and harvest control rules (HCRs).
46 The latter translate stock indicators from stock assessments into specifications for management
47 actions (*e.g.* Restrepo and Powers 1999). A successful HCR should provide an appropriate
48 response to deviations from management targets, be robust to key uncertainties, and emphasize

49 precautionary action given uncertainty. The latter point is particularly important for so-called
50 'data-poor' situations, when the reliability of stock indicators is likely questionable. Simulation
51 methods using a Management Strategy Evaluation (MSE) approach are well-developed, and
52 offer powerful tools for comparing the performance of HCRs (e.g. De Oliveira et al. 2008,
53 Butterworth and Punt 1999, Smith et al. 1999).

54 The blue eye trevalla (*Hyperoglyphe antarctica*) is a high-valued species in Australia's Southern
55 and Eastern Scalefish and Shark fishery (SESSF). The fishery for this long-lived, late-maturing
56 species is characterized by a large number of gear types operating in a range of areas, with
57 uncertainty in stock structure, apparent spatial and seasonal variability in availability of different
58 age classes, and low levels of sampling effort across the fishery (Smith and Wayte 2002, Fay
59 2007). Scientific advice for management in the SESSF takes the form of a Recommended
60 Biological Catch (RBC) for each quota species (including blue eye trevalla) for the entire
61 fishery to inform the setting of the Total Allowable Catch (TAC) (Smith et al. 2008). At present,
62 the TAC for blue eye applies across the fishery, because there are few measures in place to
63 allocate the TAC spatially¹ (a separate TAC is applied for one sector of the fishery, the trawl
64 fishery in the Great Australian Bight (GAB)).

65 The SESSF adopted a formal harvest strategy framework (HSF) as a basis for setting RBCs in
66 2005 (Smith and Smith 2005, Smith et al. 2008). This framework is based on a tier system of
67 HCRs, with the decision as to which tier a particular stock is placed in depending on the type of
68 information available on which to base a stock status determination. The tier framework is
69 intended to follow the precautionary approach, in that control rules should lead to lower RBCs,
70 and result in maintaining the stock at higher levels of spawning biomass on average as
71 information quality declines and progression through the tiers proceeds. The SESSF harvest
72 strategies specify a biomass level B_{LIM} (currently 20% of unfished spawning biomass), below
73 which targeted fishing should cease, and a target biomass B_{TARG} . The HCRs operate by
74 specifying a maximum fishing mortality rate that defines overfishing (F_{LIM}), and a target fishing
75 mortality rate that defines optimum utilization (F_{TARG}). Accounting for increasing uncertainty in
76 stock status is reflected in the application of discounts to catch – the use of which is intended to
77 achieve the same end as a decrease in the target fishing mortality rate as uncertainty about stock
78 status increases.

¹ Catches by blue eye in the trawl fishery in the Great Australian Bight (GAB) are not included in the SESSF TAC, although the catch by other gears in this area are. This is not a major sector of the fishery, catches by trawl in the GAB have been at most on the order of 1-2% of the annual total catch for blue eye in the SESSF.

79 The “Tier 3” HCR has been applied to blue eye trevalla. This HCR is designed for stocks for
80 which there exists no estimate of current biomass, but where an estimate of the current fishing
81 mortality rate, F_{CUR} , is available, most frequently from the results of catch curve analysis applied
82 to age composition data. The Tier 1 HCR is for the most information-rich case, and involves
83 calculating RBCs from the results of fitting an integrated stock assessment model (*e.g.* Stock
84 Synthesis, Methot 2007) to the available data. As the HSF was not tested before being
85 implemented, it is not clear how well the tier framework of HCRs performs, and indeed whether
86 scientific advice for management is more precautionary for species managed using the Tier 3
87 HCR, than would be the case had the species been data-rich and managed under Tier 1. Finally,
88 it is not clear how best to cope with possibly conflicting information from multiple areas and
89 gear types.

90 This paper uses MSE to assess the performance of the Tier 3 HCRs for blue eye trevalla given
91 key uncertainties. Implementation of MSE typically involves assessing the consequences of a
92 range of management options, and transparently deals with trade-offs among performance
93 criteria given a specified set of management objectives. The performance of HCRs is assessed
94 based on how well they meet management targets and objectives, including risk specifications.
95 The performance of several variants of the Tier 3 HCR that use different specifications for the
96 various reference points and/or utilize different estimation methods are compared. These
97 alternatives increase correspondence with the Tier 1 HCR, and include calculation of biomass
98 estimates and assumptions regarding the stock-recruitment relationship, negating the need for
99 the RBC to rely directly on previous year’s catch levels. HCR performance is considered both
100 when there is no spatial structuring of the population or fishery, and when there exist two
101 regions in which the fishery operates, with uncertainty related to exploitation pattern and
102 selectivity by region, and also given different assumptions regarding the spatial structure and
103 degree of mixing of the fished stock between regions.

104 Emphasis is placed on presenting key results and demonstrating HCR behaviour given different
105 approaches regarding how to improve the performance and precautionary nature of the tier
106 framework. Comparisons with data-rich scenarios are presented for some cases. While the MSE
107 is restricted to a case study of a single species and fishery, the nature of the studied resource is
108 relevant to other fished populations, and the discussion outlines general points that may be taken
109 into account when applying these methods to other systems, particularly when faced with issues
110 related to spatial uncertainty, either with respect to the resource or the fishery.

111 **3. Methods**

112 **3.1 Simulation protocol**

113 Performance of the HSF for blue eye is evaluated using a simulation modelling framework that
114 incorporates feedback between the HCR and the population dynamics. Attention is focused in
115 this section on describing the HCRs and the various modifications made to their
116 implementation, rather than describing the technical details of the operating model, which are
117 provided in full in Appendix 1. The general approach on which the operating model is based
118 consists of tuning a spatial age-structured model to represent a set of hypotheses for the
119 dynamics of the blue eye trevalla population and fishery. The values for the parameters of the
120 operating model are not based on the results of a stock assessment, as no model for the
121 population dynamics exists at present for blue eye in the SESSF. Rather, values for parameters
122 were either sourced from the literature, or derived via preliminary estimation and trial and error
123 analyses in order to mimic the general characteristics of the available data for blue eye.

124 The operating model is projected over a historical period given the known catch history for blue
125 eye, and age-composition data are generated given the known ‘true’ population. The chosen
126 HCR is then used to determine the RBC for the following year(s), given an estimation method
127 (catch curve analysis) and the selected parameters governing the HCR. The RBC is then
128 allocated to fleet and region within the operating model, the population size is updated given
129 this new catch, and additional data are generated. This assessment / population update cycle is
130 repeated for 20 years, with annual assessment and updating of the RBC. A *scenario* is defined
131 as the combination of a set of parameter values for the operating model, a data collection
132 scheme, and a specific version of the Tier 3 HCR. One hundred simulations were conducted for
133 each scenario, each differing due to process error in the population dynamics, observation error
134 when generating the age-composition data, and error associated with implementation of the
135 estimation method and application of the HCR². A series of summary statistics is calculated at
136 the end of the projection period. The summary statistics for each simulation are further analysed
137 to derive a set of performance measures, which are used to compare results among scenarios.

138 **3.2 Operating model**

139 The operating model consists of an age-structured population dynamics model that can be
140 parameterised to include spatial regions (with movement of fish among regions), and multiple
141 fleets, to capture key dynamics for blue eye trevalla. Full technical specifications for the
142 operating model are detailed in Appendix 1. Analyses detailed in this chapter consider two

² The results obtained from 100 simulations were almost identical to those obtained when 1,000 simulations were used to characterise a scenario for a subset of the scenarios described.

143 versions of the operating model: (a) a single population occupying a single region and exploited
144 by a single fishing fleet, and (b) a population occupying two regions with movement between
145 regions, and exploited by one or two fishing fleets (with different selectivity patterns). Several
146 parameterizations of each version of the operating model are considered to investigate the
147 implications of key uncertainties. The parameterization of the operating models, along with the
148 values for biological parameters for blue eye considered for the various scenarios, are given in
149 Tables 1 and 2, and Figure 1.

150 Scenarios using the two-region version of the model are designed to mimic general assumptions
151 regarding the nature of the blue eye trevalla fishery, rather than the actual spatial structure. Two
152 ‘continental slope’ regions with differing exploitation histories are assumed, with levels of stock
153 mixing between the two regions, ranging from full mixing, in that the impacts of spatial
154 variability are minimal, to almost no mixing, indicating a high degree of spatial structuring in
155 the blue eye population. Spatial differences in population responses to exploitation are more
156 likely to be observed under the latter scenario. The regional catch histories used to drive the
157 population dynamics (Figure 1f) are taken from the landings data from the relevant zones of the
158 SESSF, with the geographic split in these data being catches taken east and west of Tasmania.

159 **3.3 Harvest strategies**

160 The harvest strategies consist of a data collection scheme, a method to estimate the current
161 fishing mortality rate F_{CUR} , and an HCR. Scenarios are limited to instances where the harvest
162 strategy is applied every year of the projection period, consistent with the current practice of
163 annual setting of TACs within the SESSF. The two forms for the Tier 3 HCR shown in Figure 2
164 are tested, with two methods for estimating F_{CUR} . Variations of the HCR that utilise different
165 reference points and have differing data requirements are implemented as outlined below.

166 **3.3.1 Data and estimation methods**

167 Data available for the Tier 3 analyses were limited to fishery-dependent age-composition data
168 (*i.e.* no index of abundance or fishery-independent data), with an annual multinomial sample
169 size of 100 allocated by fleet and region in the same proportions as the annual catch (*i.e.* the
170 total sample size was 100). While this sample size is a good deal less than the number of otoliths
171 that have been aged annually in recent years for blue eye (on the order of 500 per year), it is
172 perhaps unreasonable to think that these data truly constitute a random sample of size equal to
173 the number of aged otoliths (e.g. Candy 2008, Miller and Skalski 2006). A random sample of
174 100 represents a reasonably good sample size that might be hoped for from SESSF species.
175 Evaluation of HCR performance when sample size is reduced or not randomly determined from
176 the catch is not considered in this chapter. Four years of age-composition data were assumed to

177 be available to the estimators. Two catch curve estimation methods were employed: (a) the
 178 Chapman and Robson (1960) catch curve estimator (CR), and (b) a multi-year equilibrium F
 179 age-structure based-estimator (MYEF). The estimators aim to estimate total mortality, Z , with
 180 estimation of F then achieved given an assumed value for the rate of natural mortality, M
 181 (denoted “assumed M ” in Tables 1 and 2). For the CR method, catch curves were applied to the
 182 annual age-composition data, with F_{CUR} calculated as an inverse-variance weighted average of
 183 the annual estimates. In contrast, MYEF integrates over all years, therefore averaging over years
 184 is not required to obtain an estimate of F_{CUR} for this estimation method.

185 *a) Chapman and Robson catch curve estimator (CR)*

186 The CR estimator assumes that the population is in equilibrium, and that recruitment is constant
 187 over time. The estimate of Z , from a sample of the age composition for a given year is:

$$188 \quad Z_y = \ln \left(\frac{1 + \bar{a}_y - 1/n_y}{\bar{a}_y} \right) \quad (1)$$

189 where \bar{a}_y is the mean age (above the recruitment age) of the sample and n_y is the sample size
 190 for year y . A single estimate of Z is required to calculate the RBC, and so weighted averages of
 191 estimates of Z_y from the most recent four years of age-composition data were calculated, with
 192 weighting inverse to the variance estimate for each year:

$$193 \quad \text{Var}(Z_y) \approx \frac{(1 - e^{-Z_y})^2}{n_y e^{-Z_y}} \quad (2)$$

194 Catch curve estimators are known to be sensitive to the age-range of the data used (Chapman
 195 and Robson 1960, Dunn et al. 2002). For the analyses presented here, the recruitment age was
 196 set at that for which the numbers-at-age were greatest, with the maximum age being determined
 197 from the sample. CR assumes uniform selectivity for ages above the recruitment age, likely
 198 biasing estimates of vulnerable biomass when selectivity is actually dome-shaped.

199 *(b) Multi-year equilibrium F age-structure based-estimator (MYEF)*

200 Estimation of F_{CUR} using MYEF involves fitting an equilibrium-based age-structured population
 201 dynamics model to the available age-composition data, with the population model being of the
 202 form:

$$N_a = \begin{cases} 1 & \text{if } a = 0 \\ N_{a-1}e^{-(s_{a-1}F+M)} & \text{if } 0 < a < 100 \\ \frac{N_{a-1}e^{-(s_{a-1}F+M)}}{(1 - e^{-(s_a F+M)})} & \text{if } a = 100 \end{cases} \quad (3)$$

where the N_a 's are the numbers-at-age, s_a is the (estimated) selectivity at age (assumed to be asymptotic and to follow a logistic curve), F is the estimated rate of fishing mortality, and M is the assumed rate of natural mortality. The values for F and the parameters which define s_a are determined by maximizing the following log-likelihood function:

$$\ln L = \sum_y n_y \sum_a O_{y,a} \ln \left(\frac{\tilde{N}_a}{O_{y,a}} \right) \quad (4)$$

where $O_{y,a}$ is the observed proportions in the sample by age in year y , n_y is the sample size for year y , and \tilde{N}_a are the predicted proportions of catch-at-age:

$$\tilde{N}_a = \bar{N}_a / \sum_{a'} \bar{N}_{a'} \quad (5)$$

$$\bar{N}_a = \frac{N_a s_a F}{(s_a F + M)} (1 - \exp^{-(s_a F + M)})$$

Maximisation of (4) was achieved using AD Model Builder (ADMB Project 2009). Differences between MYEF and CR are that MYEF accounts for selectivity, data from all ages are used, and the likelihood is multinomial. Unlike the CR estimator, no averaging of annual mortality estimates is necessary to calculate the RBC under MYEF because F is calculated using all the available data simultaneously.

The scenarios outlined in Tables 1 and 2 include uncertainties related to applying the estimation methods. Importantly, the impact of assuming the incorrect value for M when conducting the estimation is examined.

3.3.2 Harvest Control Rules

Concern about the performance of the Tier 3 HCR has been noted following implementation (Klaer et al. 2009). There is concern that the original nature of the calculation of RBCs for Tier 3 (applying an appropriate multiplier to recent average catch levels, Figure 2b) could produce a ratchet effect of continually increasing or decreasing catches, even though information suggests that the target level has been reached. A revised harvest control rule (Klaer et al. 2009), which shows consistency with the more data-rich tier rules in terms of reference points, was applied in

227 2008 (Figure 2c). Unlike the ‘old’ rule, this ‘new’ rule does not have a cap on annual catch
 228 increases.

229 Each of the scenarios outlined in Table 1 were projected using three variants of the Tier 3 HCR
 230 (Figure 2), which differed either by adopting the ‘old’ or ‘new’ Tier 3 rule, and in the choice for
 231 the target and limit reference points:

- 232 1. The shape of the HCR follows the ‘old’ rule (Figure 2b), with $F_{TARG} = M$,
- 233 2. The shape of the HCR follows the ‘new’ rule (Figure 2c), with $F_{TARG} = 0.5M$ and $F_{LIM} = M$,
 234 and
- 235 3. As for 2), but with the reference points adopting a Tier 1-like approach with $F_{TARG} = F_{40}$,
 236 and $F_{LIM} = F_{20}$. (F_{40} and F_{20} are the fishing mortality rates which will result in [under
 237 equilibrium age structure] spawning biomasses of 40% and 20% of unfished spawning
 238 biomass [corresponding to the B_{MSY} proxy and B_{LIM} under the SESSF Tier 1 HCR]).

239 The values for M used in the HCRs (and that used to calculate F) are the ‘assumed M ’ values as
 240 detailed in Tables 1 and 2.

241 Empirical investigation suggests that the assumption of $F_{MSY} \approx M$ is too high for blue eye
 242 trevalla (Figure 3). Walters and Martell (2004) suggest $F_{msy} = cM$, with values for c including
 243 0.8 in general, but 0.6 or less for commonly fished species (Walters and Martell 2004). For U.S.
 244 west coast groundfish species, the average is $c = 0.62$ (MacCall 2007), and so $0.5M$ was chosen
 245 for the analyses here to adopt a conservative estimate.. Calculation of F_{40} and F_{20} depends on the
 246 values for the parameters of the stock-recruitment relationship (assumed to follow a Beverton-
 247 Holt form), and requires estimates of the steepness parameter h (Mace and Doonan 1988),
 248 information on growth and fecundity, and selectivity in addition to an estimate of M . The values
 249 for these reference points used in the HCR were calculated based on the estimates of selectivity
 250 from the estimators, an assumed value for h of 0.75, and the ‘correct’ values for growth and
 251 fecundity (Figure 1a-c). In contrast, versions 1) and 2) of the Tier 3 HCR rely only on an
 252 estimate of M to calculate the RBC given F_{CUR} . However, version 3) more appropriately
 253 accounts for biology when determining the likely response to fishing.

254 Calculation of the RBC under version 1) is achieved by applying the appropriate multiplier from
 255 Figure 2b to C_{cur} , defined as the average catch over the four years prior to the year for which an
 256 RBC is needed. Under versions 2) and 3), the RBC is calculated by first obtaining F_{RBC} given
 257 Figure 2c, and applying the formula:

258
$$RBC = C_{cur} YPR(F_{RBC}) / YPR(F_{cur}) \quad (6)$$

259 where $YPR(F)$ is the yield-per-recruit obtained given a fishing mortality F . Note that equation
 260 (6) allows for greater increases in catch than does the old Tier 3 HCR (maximum increase of
 261 20% above the recent average, Figure 2b), if F_{CUR} is estimated to be below the target level.
 262 Irrespective of this, the maximum allowable change in the catch (RBC) from one year to the
 263 next was restricted to 50%³.

264 Comparison of Tier 3 performance with that expected under Tier 1 is achieved by calculating
 265 the projected spawning stock biomass trajectories for a subset of the scenarios in Table 1 under
 266 the Tier 1 HCR. This involved generating additional data (cpue (20 yrs, CV=0.3), and length
 267 composition (10 years, $n_y=100$)), and applying Stock Synthesis 2 (Methot 2007) to this data set
 268 each year of the projection period. Results for Tier 1 HCR are simply shown for comparison
 269 purposes because the focus of this chapter is the Tier 3 HCRs.

270 **3.3.3 Accounting for fleet/spatial structure**

271 Uncertainty in spatial structure through the scenarios in Table 2 presents additional challenges
 272 when implementing the Tier 3 HCRs, because of the need for decisions regarding what
 273 combinations of fleet and region are to provide the parameters used when calculating the RBC,
 274 and how to choose among potentially differing estimates of the fishing mortality rate. The
 275 scenarios in Table 2 were crossed with the following options to investigate how performance
 276 given spatial structure changes with assumptions regarding how the data are analysed:

- 277 1. spatial complexity is ignored, and a single analysis (CR, MYEF) is conducted using the data
 278 pooled across regions (added together as samples are allocated by region relative to the size
 279 of the catch) – this is how the Tier 3 control rule is applied in the SESSF at present,
- 280 2. the data from the two regions are analysed separately to obtain two estimates of current
 281 fishing mortality / stock status; these estimates are then weighted by the inverse of their
 282 variance estimates to obtain the RBC.
- 283 3. separate analyses as in 2, but the maximum estimated F is used to calculate the RBC.

284 The variance estimates for F_{CUR} are (primarily) driven by sample size, and so option 2
 285 effectively weights the regional estimates by the current catch allocation. Option 3 is potentially
 286 more conservative because it bases the RBC on the parameters for the region with the highest
 287 estimated fishery mortality rate. However, this option can be expected to be more prone to
 288 inaccurate estimates of F that might result from low sample sizes.

³ Within the HSF of the SESSF, a rule exists where the TAC for quota species cannot change by more than 50% from one year to the next.

289 **3.4 Performance measures**

290 Performance of the HCRs is evaluated using a set of performance measures:

- 291 1. The median (over simulations) spawning stock status at the end of the projection period
292 (final spawning biomass as a fraction of unfished spawning biomass, B_0), [median final
293 depl.].
- 294 2. The inter-quartile range of the spawning stock status (relative to B_0) at the end of the
295 projection period [IQR final depl.].
- 296 3. The probability of the spawning biomass being below the Tier 1 limit reference point (B_{20})
297 at the end of the projection period [$P(\text{final } B < B_{LIM})$].
- 298 4. The probability of the spawning biomass going below the Tier 1 limit reference point (B_{20})
299 at some point during the projection period [$P(B < B_{LIM} \text{ anytime})$].
- 300 5. The median of the average annual catch during the projection period [median (avg. TAC)].
- 301 6. The median (over simulations) of the CV of the annual catches during the projection period
302 [median(CV TAC)].
- 303 7. The mean (over simulations) number of years for which the RBC is less than $4t^4$ [mean(#yrs
304 collapse)].

305 Performance measures 1-4 relate to the effect of implementing the HCR on spawning biomass,
306 while measures 5-7 provide information regarding the catch performance of the HCR.

307 **4. Results**

308 The results of the simulations are displayed in the form of boxplots of the performance measures
309 across scenarios to compare among the HCRs and methods for obtaining F estimates. Simple
310 linear models are used to evaluate the contribution of the different scenario specifications to the
311 values for the performance measures. The scenario characteristics as defined in Tables 1 and 2,
312 the catch curve estimation type, the choice of HCR, and (for the spatial analyses) the method for
313 obtaining a single F estimate, were included as factors in the linear predictors of these models,
314 fitted separately for the seven performance measures. Interaction terms involving some of the
315 factors were also considered.

316 **4.1 Non-spatial analyses**

317 The performance of the three versions of the Tier 3 HCRs, given estimation using CR and
318 MYEF, are compared in Figure 4. The old Tier 3 HCR leads to levels of spawning biomass that
319 are well below the Tier 1 target and limit biomass reference points (40 and 20% of unfished

⁴ $4t$ is 1% of the total catch prior to implementation of the harvest strategy, this performance measure is intended to reflect the frequency of fishery collapse.

320 spawning biomass) at the end of the projection period, (Figure 4a) with high probabilities of
 321 dropping below B_{20} during the projection period (Figure 4d). The performance of the new HCR
 322 varies considerably among scenarios and the projections under this HCR lead to more variable
 323 catches (Figure 4f). However, the results for this HCR are generally more optimistic regarding
 324 stock status (Figure 4a, 4c), although many scenarios still remain below the target biomass at the
 325 end of the projection. Comparison of performance for three scenarios suggests that, for these
 326 scenarios at least, the Tier 3 HCRs are not precautionary compared to the Tier 1 HCR, because
 327 the Tier 1 HCR leads to higher relative biomass, a lower probability of dropping below the limit
 328 reference biomass, and lower, less variable annual catches (Figure 5).

329 The changes in performance with respect to final stock status, the risk of going below the limit
 330 reference point, and the magnitude in catch levels are largely independent of the estimation
 331 method (CR versus MYEF), but are a function of the HCR (Table 3, 'new HCR' rows).
 332 Adopting $F_{TARG}=F_{40}$ and $F_{LIM}=F_{20}$ results in an increase in the median final relative spawning
 333 biomass (Table 3, new HCR, Figure 4a). The differences between applying the old and new
 334 HCRs, for the two estimation methods can be seen clearly in Figure 4, which shows the
 335 distribution of the values for the performance measures across all of the scenarios in Table 1.

336 Performance of the new Tier 3 HCR is also determined by the choice of reference points. The
 337 HCR based on the spawner-recruitment reference points ($F_{TARG}=F_{40}$ and $F_{LIM}=F_{20}$) tend to lead
 338 to higher values for relative spawning biomass, lower probabilities of dropping below the limit
 339 reference point, and lower median annual catches than the $F_{TARG}=0.5M$ version of the new Tier
 340 3 HCR (Figure 4a, c-e). However, performance is variable among scenarios, and the probability
 341 of dropping below the limit biomass remains very high for a number of the scenarios (Figure 4c-
 342 d).

343 Variability in the values obtained for the performance measures was caused not only by the
 344 choice of HCR. Scenarios where the true value for steepness was low (" $h=0.3$ ") resulted in
 345 lower final biomass, an increased probability of dropping below B_{LIM} , and increased variability
 346 in the annual catches (Table 3). Likewise, more productive stocks (" $h=1.0$ ") resulted in higher
 347 final biomass levels and a lower probability of being below the limit reference point at the end
 348 of the projection period. Scenarios in which the initial (prior to implementation of the HCR)
 349 relative stock size was low (" $InitDepl=0.2$ ") resulted in lower levels of catch (albeit more
 350 variable). Under the old Tier 3 HCR, a higher initial stock size (" $InitialDepl=0.75$ ") led to
 351 higher catches, an increase in the final relative stock size and a lower probability of being below
 352 the limit reference point at the end of the projection period. However, an interaction between the
 353 initial stock size and the choice of HCR meant that under the new HCR, scenarios starting at

354 high relative biomass resulted in large, unsustainable catches being taken, and a general poor
 355 performance of the HCR in terms of maintaining stock status, and near ubiquitous probability of
 356 ending the projection below the limit biomass (Table 3, “new HCR : Init Depl interactions”).
 357 This change in behavior between the old and new Tier 3 HCR for the high initial stock size
 358 scenarios was largely a result of the difference in maximum allowable increases in catch (old
 359 Tier 3 has a cap of 20% increase versus 50% for the new HCR).

360 In terms of magnitude, aside from the initial stock size, the factor with the largest impact on the
 361 biomass-related performance measures was whether the assumed value for M was correct or not.
 362 Assumed values for M less than the true value resulted in more optimistic outcomes in terms of
 363 stock status, with higher final biomasses, and lower probabilities of dropping below the limit
 364 reference point (Table 3, ‘assumed $M < \text{true } M$ ’). Average catches were also lower. Conversely,
 365 assuming a value for M greater than the true value resulted in an under-estimation of F , and
 366 consequently, outcomes with lower final relative biomass and a higher risk of dropping below
 367 the limit (Table 3, ‘assumed $M > \text{true } M$ ’).

368 **4.2 Spatial analyses**

369 The results for the ‘spatial’ two-region scenarios for the $F_{\text{TARG}}=F_{40}$ version of the new Tier 3
 370 HCR are shown in Table 4, and include results for the three options related to how to deal with
 371 the spatial data (see Section 3.3). Results for this implementation of the HCR (new form,
 372 $F_{\text{TARG}}=F_{40}$) are shown because this option appeared to best satisfy management objectives in the
 373 non-spatial analyses described above. A decrease in the connectivity of the regions results in a
 374 decrease in the probability of dropping below B_{20} , and increases in final spawning depletion for
 375 scenarios when the stock is initially at the biomass target (Table 4, F option 1). This is
 376 presumably because the decrease in movement between regions increases the signal in the data,
 377 as the initially exploited region must be driven to low levels before implementation of the
 378 harvest strategies. However, this sensitivity to the degree of connectivity is lost when the initial
 379 spawning depletion is either at high or low levels (Table 4, scenarios 1-7). The initial status of
 380 the stock therefore appears to be at least as important (if not more so) in determining the values
 381 for the performance measures as the connectivity among the regions. Indeed, the results of linear
 382 modeling to predict the values of performance measures suggests that the effect of the degree of
 383 mixing between regions is not important (Table 5).

384 There was no impact of moving from the intermediate (in which the average mixing rate is 20%)
 385 to the limited (5%) level of mixing (the magnitudes of the coefficients for the intermediate and
 386 limited mixing scenarios given a particular performance measure were almost the same). The
 387 age structure of fish mixing between regions appeared less important in driving performance.

388 Whether selectivity was dome-shaped, or modelled differently by region was a major
389 determinant of performance, with the amount of dome-shaped selectivity (in 1 region or 2)
390 leading to higher final relative spawning biomasses and lower probabilities of going below the
391 B_{20} limit (Table 4 and Table 5, scenarios 8-9, 'Different selectivities by region' and 'Selectivity
392 dome-shaped in both regions'). Lower catches resulted from selectivity being dome-shaped in
393 both regions (Table 5, 'Selectivity dome-shaped in both regions').

394 Analysing the data by region and then choosing the maximum estimated F to set the RBC
395 (Table 4, F option 3) unsurprisingly led to the most optimistic results regarding spawning stock
396 biomass, and the probability of going below the limit reference point (Figure 6). This choice
397 also resulted in tighter intervals for the biomass. The relative performance of the different
398 scenarios is very similar when data from both regions are analysed together and when the
399 regional estimates are weighted by their variance (Table 4, F options 1 and 2), although the
400 latter case appears more variable. An exception is when movement between regions is limited to
401 pre-recruits (Table 4, scenario 8). In this instance, aggregating the data and conducting a single
402 analysis appears to be a much more conservative way to determine RBCs, because the relative
403 biomass is well below B_{20} when regional estimates of F are weighted by the inverses of their
404 variances. As with the non-spatial analyses, a large proportion of the variation in the
405 performance measures among scenarios can be attributed to the relative stock size prior to
406 implementing the harvest strategy, rather than the specifications for the particular HCR
407 implemented. The increase in final biomass and decrease in the risk of dropping below B_{20}
408 associated with choosing the maximum regional F estimate are naturally associated with lower
409 catches, however do not result in a decrease in variability in catches, nor a decrease in the
410 relative frequency of fishery collapse (Figure 6f-g). This option also appears to mitigate the
411 change in performance associated with the spatial connectivity among regions, as the values for
412 the performance measures do not change with decreasing connectivity as for the case when the
413 regional data are aggregated prior to analysis (Table 4, compare scenarios 1,2, and 5 between F
414 options 1 and 3). This suggests the degree to which sampling error has on the performance of
415 the HCR, as for scenario 1, the true exploitation rate is the same in both regions yet F option 3
416 results in higher final spawning stock biomass.

417 Although the results suggest that reasonable performance can be achieved using the new Tier 3
418 HCR given an appropriate choice of reference points and decision rule for dealing with space (at
419 least compared to the original Tier 3 HCR), Figure 7 suggests that performance of these HCRs
420 is not particularly satisfactory, because higher relative spawning biomass may be a result of
421 closing the fishery for a number of years following a series of successive increases (or
422 decreases) in the RBC. This is also reflected in the values for the mean number of years in

423 which the fishery collapses (Figure 4g, Figure 5g, Figure 6g). The trajectories in Figure 7
424 suggest, as inferred above, that for a species like blue eye, the catch curve is fairly unresponsive
425 in detecting changes in F . This can be expected for a long-lived species, where there would
426 presumably be considerable inertia in the age structure. As such, the estimates of F obtained
427 may not be reflecting the current fishing mortality rate.

428 **5. Discussion**

429 Management based on rapid stock assessment is attractive for fisheries where there are limited
430 data, and methods for such assessment, including catch curve analysis, are well-established
431 (albeit also with well-known shortcomings related to unrealistic assumptions). The MSE testing
432 of the Tier 3 HCRs presented here suggests that it is indeed possible to formulate HCRs based
433 on the results of catch curves that address management objectives (i.e. maintain spawning stock
434 biomass at or above target levels), despite some of these shortcomings. However, it is also clear
435 that implementing the Tier 3 HCRs can result in undesirable behaviour, and that outcomes can
436 be sensitive to many of the known shortcomings of the associated estimation methods.

437 Assessing performance of the HCRs through their ability to conserve stock biomass may not be
438 an appropriate choice – the spawning biomass trajectories in Figure 7 suggest that satisfactory
439 outcomes for a scenario (for example, a low probability of being overfished) can be achieved
440 with undesirable system properties (such as complete closure of the fishery following a
441 ratcheting increase in catch), even for the “new” Tier 3 HCR. Klaer et al. (2009) and Smith et
442 al. (2008) address issues related to the unresponsiveness and ratcheting behaviour of the Tier 3
443 HCR. These undesirable properties are likely to be more pronounced for longer-lived species
444 because the catch curve does not relate to current conditions. Unresponsiveness in the Tier 3
445 HCR is also a consequence of restrictions on the magnitude of permitted changes in
446 management actions (the RBC is only allowed to change by 50% in a given year even if the
447 estimate of F changes dramatically). The results suggest that such a behaviour appears to result
448 in higher final biomass levels for stocks that are at low relative stock size prior to
449 implementation of the HCRs compared with those achieved for stocks that are at or above
450 management targets Table 3 and Table 5). Increasing the time period over which the catch is
451 averaged will mitigate the ratcheting effect of RBCs (concurrent increases or decreases),
452 however doing so effectively downweights the influence of previous management actions.

453 Differences in the performance of the Tier 3 HCRs appeared to be related to both the form of the
454 HCR, and the values chosen for the reference points (e.g. Figure 4). Tier 3 HCRs that used the
455 spawner-recruit-based reference points resulted in the best perceived performance (Figure 4).
456 However, performance of the rules using a target of $0.5M$ was generally only marginally

457 different than those using spawn-recruit-based reference points, even though the data
458 requirements were markedly less (Table 3 and Figure 4). As estimates of M already tend to be
459 uncertain (with results being very sensitive to assuming the wrong value), including additional
460 uncertainty associated with estimating the compensation of the spawner-recruit curve
461 (steepness) is perhaps unnecessary. However, Figure 3 clearly shows that $0.5M$ is not
462 necessarily an appropriate target rate of fishing mortality (when compared with Tier 1 reference
463 points) for all instances (*e.g.* when steepness is low). Note that even the ‘poorly’ performing
464 HCRs require an estimate of M , typically derived from longevity and growth information (*e.g.*
465 Hoenig 1983, Jensen 1996, Pauly 1980). While such information generally tends to be available,
466 the nature of a ‘data-poor’ fishery may mean that these estimates are uncertain. The CV of M
467 estimates from the Pauly and Hoenig methods are 0.53 and 0.61 respectively (MacCall 2009),
468 and therefore it might be unreasonable to assume greater certainty in M than this for a data-poor
469 stock (MacCall 2009 recommends a CV of at least 0.5).

470 The results clearly demonstrate the need for careful application of ‘common sense’ when
471 applying methods such as the Tier 3 HCRs. For example, the implications of dome-shaped
472 selectivity are that mortality is over-estimated, leading to specification of lower catches, but it
473 would be somewhat foolish to use this conservation of stock biomass as a reason for
474 implementation of the Tier 3 HCRs when selectivity is known to be dome-shaped. Having an
475 accurate estimate for M appears to be very important for HCR performance, with scenarios
476 where the chosen value for M is higher than the true value resulting in high probabilities of
477 dropping below the limit reference point. Similarly, scenarios for which the assumed value for
478 M is lower than the true value are among the most conservative in terms of biomass relative to
479 the unfished state at the end of the projection. These results are unsurprising, as the estimate of
480 F is clearly negatively correlated with M . The impact of selectivity being dome-shaped is
481 similar to that of under-estimating M , in that F is over-estimated (because the estimators assume
482 selectivity to be asymptotic), resulting in lower RBCs and higher spawning stock biomasses.

483 Although the analyses examined the impact of collecting data from multiple regions, and where
484 the regional allocation of catches was changing, the data were generated in proportion to the
485 catch, with no over-dispersion or bias in the sample other than the stochasticity imposed on the
486 data through sample size and multinomial sampling. The low sampling effort present in the
487 actual blue eye data set, coupled with seasonal differences in availability, means that the age and
488 length data are not representative of the fishery as a whole. Indeed, the sample size of the age
489 data for blue eye is such that pooling age data across years to obtain an age-length-key and then
490 applying this to the year/region-specific length composition data is the most likely means of
491 estimating the age-composition of the catch (*e.g.* Klaer 2008). While the analyses investigating

492 the impacts of region-specific selectivity go some way to addressing these questions, it is likely
493 that incorporation of bias and non-representative sampling into the MSE framework will further
494 degrade HCR performance. It is also not clear how the way in which future catches are allocated
495 by region/fleet impacts the results of this paper. The lack of difference between scenarios that
496 varied in the degree of spatial connectivity can be attributed somewhat to the allowance of a
497 shortfall in the catch in one region (as a result of insufficient available biomass) to be taken in
498 the other region if required.

499 Most fisheries and also fished populations exhibit spatial structure, creating spatial
500 heterogeneity in realized exploitation rates and biomass trends, with the extent of heterogeneity
501 depending on the level of mixing in the stock. However, most management agencies lack the
502 ability (or rather, the infrastructure) to specify the TAC at the level of this spatial structuring.
503 HCRs that show robustness to spatial differences are therefore desirable. Disaggregating the
504 data by fleet and region, analyzing these data separately, and then choosing the maximum
505 estimate of F to determine the RBC appears to produce the most conservative results
506 irrespective of the true nature of stock connectivity and fishery behaviour, and also resulted in
507 the most consistent values for the performance measures among scenarios that varied in spatial
508 structure. However, application of this version of the HCR leads to perhaps unnecessarily low
509 catches when the connectivity of the stock between regions is high, and reflects the impact that
510 sampling error can be expected to have on HCR performance in such scenarios. The maximum
511 F option would also be inappropriate if the maximum F estimate came from a sector of the
512 fishery which was a minor component of the catch, as it would be more likely that such an F
513 estimate would be both uncertain and not representative of the overall exploitation rate.
514 Weighting fleet and regional estimates of F by their variance accounts for this if the data are
515 collected proportionally with the catch, as was implemented here. If not, then additional rules to
516 determine how to proceed will be needed. For example, weighting the F estimates by catch
517 rather than variance. Such methods however will not accommodate the effects of dome-shaped
518 selectivity have on over-estimation of F . Spatial disaggregation of data that already has low
519 sample size will result in more variable estimates of mortality than might be expected given
520 population dynamics, particularly when constructing annual catch curves.

521 The use of an MSE approach enables the examination of control rules used to set catch limits,
522 by evaluating performance given the known true state of the system. Such a framework can be
523 used to identify strategies that perform poorly in the fairly well-ordered structure of the
524 simulation. Perhaps more importantly, the relative performance of different strategies can be
525 compared. The adoption of a precautionary approach to management of exploited marine
526 resources is increasingly common, and it is clear that testing of harvest control rules is necessary

527 to understand whether these rules can be expected to perform as intended. The analyses
528 described focus on parameterizations of the operating model which mimic blue eye trevalla, but
529 the system can be extended to examine the performance of the tier framework given different
530 life histories. Indeed, a natural avenue for further extension of these analyses would be to
531 examine whether the relative performance of the various Tier 3 control rules depends on the life-
532 history of the species of interest, and whether the various HCRs need to be modified with life
533 history.

534 While improved performance and conservation of stock biomass is achieved under the new Tier
535 3 HCR over that of the old form, the variability around the stock biomass, and in catches under
536 this HCR are greater than that expected for a more data-rich scenario (e.g. integrated assessment
537 using Stock Synthesis). This is to be expected; data-poor methods should estimate quantities of
538 interest with greater uncertainty than those for which more data are available. While the Tier 3
539 HCR based on reference points such as F_{40} and F_{20} is more equivalent to the Tier 1 HCR, care
540 should be taken regarding the ability to estimate F sufficiently well to be able to apply this rule
541 successfully. Application of these reference points under the Tier 3 HCR requires an estimate of
542 the value for steepness, which cannot be obtained during the analysis and was assumed to be
543 0.75 regardless of the true value. Consequently, performance of the HCRs was poor when the
544 true value for steepness was lower than this. However, the approach taken here is not much
545 different than that employed for data-rich scenarios in the SESSF, as estimation of steepness
546 within stock assessments for this fishery is restricted to the assessments for tiger flathead
547 (*Neoplatycephalus richardsoni*, e.g. Klaer 2010) and eastern gemfish (*Rexea solandri*, Little and
548 Rowling 2009). In general, although the new Tier 3 HCR only relies on one source of current
549 data from the fishery, application of the HCR requires estimates be available for the majority of
550 biological parameters that would be included in a more formal stock assessment based on a
551 statistical catch-at-age model. The performance of such estimators (e.g. Stock Synthesis) given
552 paucity of information, the robustness of such models to mis-specifications such as those
553 investigated here, and comparison of performance with the Tier 3 HCRs warrants interest.

554 The desired F to be estimated is the current rate of fishing mortality, whereas the annual catch
555 curve integrates over the fishing mortality rates experienced by the stock for the length of the
556 age structure, which may either not correspond well with recent trends in F , or, if data are noisy,
557 may impede estimation of F . Poor ability to estimate F may mean a lack of ability to truly
558 discriminate between the reference points involved in the HCR. This may be particularly
559 important for long-lived, late-maturing species where F_{40} and F_{20} are similar. Successful
560 implementation of a harvest control rule relies on being able to distinguish between values for
561 stock indicators that result in changes in management action. Approximate confidence intervals

562 for the current rate of fishing mortality on blue eye trevalla based on application of the MYEF
 563 estimator to data from the auto-longline fishery are wider than the range of F 's over which
 564 changes in management actions are indicated given the HCR (Fay 2009).

565 Precaution with respect to Tier 1 is not explicitly built into the Tier 3 HCR at present,
 566 particularly as the quantities for F_{TARG} and F_{LIM} are the same as for Tier 1 (even though their
 567 estimates may be different). Conservation of stock biomass under the Tier 3 HCR arises from
 568 the behaviour of the rules. Additional measures to modify the Tier 3 HCR such that there is
 569 equivalency of risk with the Tier 1 HCR could involve the choice of alternative reference points
 570 (e.g. $F_{TARG} = F_{50}$), the application of a discount to the RBC for being at a less data-rich tier level
 571 (Smith et al. 2008), or perhaps application of current HCRs with a more conservative value for
 572 F_{CUR} , based on some percentile of the confidence interval of the estimate. Further simulation
 573 testing to address the efficacy of such approaches is clearly warranted, and is a suitable
 574 candidate for future work.

575 **6. Acknowledgements**

576 Funding for GF was provided by CSIRO Marine and Atmospheric Research as part of the
 577 SESSF stock assessment project. The members of the SESSF stock assessment team, J. Day, M.
 578 Haddon, N. Klaer, R. Little, R. Thomson, G. Tuck, J. Upston, and S. Wayte, are thanked for
 579 extensive discussions and input.

580 **7. References**

- 581 ADMB Project. 2009. AD Model Builder: automatic differentiation model builder. Developed
 582 by David Fournier and freely available from admb-project.org.
- 583 Butterworth, D. S., K. L. Cochrane, and J. A. A. De Oliveira. 1997. Management Procedures: a
 584 better way to manage fisheries? The South African experience. Pages 83-90 in E. L.
 585 Pikitch, D. D. Huppert, and M. P. Sissenwine (Eds). Global trends: Fisheries
 586 Management. American Fisheries Society, Symposium 20, Bethesda, Maryland.
- 587 Butterworth, D. S. and A. E. Punt. 1999. Experiences in the evaluation and implementation of
 588 management procedures. ICES Journal of Marine Science 56: 985-998.
- 589 Candy, S. G. 2008. Estimation of effective sample size for catch-at-age and catch-at-length data
 590 using simulated data from the Dirichlet-multinomial distribution. CCAMLR Science 15:
 591 115-138.
- 592 Chapman, D. G. and D. S. Robson. 1960. The analysis of a catch curve. *Biometrics* 16: 354-368.
- 593 Cooke, J. G. 1999. Improvement of fishery-management advice through simulation testing of
 594 harvest algorithms. ICES Journal of Marine Science 56: 797-810.

- 595 Dunn, A., R. I. C. C. Franics, and I. J. Doonan. 2002. Comparison of the Chapman-Robson and
596 regression estimators of Z from catch-curve data when non-sampling stochastic error is
597 present. *Fisheries Research* 59: 149-159.
- 598 De Oliveira, J. A. A., L. T. Kell, A. E. Punt, B. A. Roel, and D. S. Butterworth. 2008. Managing
599 without best predictions: the Management Strategy Evaluation framework. Pages 104-
600 134 in *Advances in Fisheries Science; 50 years on from Beverton and Holt*. Blackwell
601 Publishing. Oxford.
- 602 Fay, G. 2007. Tier 3 calculations for blue eye trevalla (*Hyperoglyphe antarctica*) using data up
603 to and including 200. Pages 524-531 in Tuck, G. N. (ed.) 2007. *Stock Assessment for the*
604 *Southern and Eastern Scalefish and Shark Fishery 2006-2007*. Volume 1: 2006.
605 Australian Fisheries Management Authority and CSIRO Marine and Atmospheric
606 Research, Hobart. 577 p.
- 607 Fay, G. 2009. Tier 3 calculations for blue eye trevalla (*Hyperoglyphe antarctica*) using data up
608 to and including 2007. Pages 211-225 in Tuck, G. N. (ed.) 2009. *Stock Assessment for*
609 *the Southern and Eastern Scalefish and Shark Fishery 2008*. Part 2. Australian Fisheries
610 Management Authority and CSIRO Marine and Atmospheric Research, Hobart. 331 p.
- 611 Hoenig, J. M. 1983. Empirical use of longevity data to estimate mortality rates. *Fishery Bulletin*
612 82: 898-903.
- 613 Jensen, A. L. 1996. Beverton and Holt life history invariants result from optimal trade-off of
614 reproduction and survival. *Canadian Journal of Fisheries and Aquatic Sciences* 53: 820-
615 822.
- 616 Kell, L. T., C. M. O'Brien, M. T. Smith, T. K. Stokes, and B. D. Rackham. 1999. An evaluation
617 of management procedures for implementing a precautionary approach in the ICES
618 context for North sea plaice (*Pleuronectes platessa* L.). *ICES Journal of Marine Science*
619 56: 834-84
- 620 Kell, L. T., M. A. Pastoors, R. D. Scott, M. T. Smith, F. A. Van Beek, C. M. O'Brien, and G. M.
621 Pilling. 200. Evaluation of multiple management objectives for Northeast Atlantic flatfish
622 stocks: sustainability vs. stability of yield. *ICES Journal of Marine Science* 62: 1104-
623 1117.
- 624 Klaer, N. L. 2008. Yield and total mortality values and Tier 3 estimates for selected shelf and
625 slope species in the SESSF 2008. In Tuck, G.N. (ed.) 2009. *Stock Assessment for the*
626 *Southern and Eastern Scalefish and Shark Fishery 2008*. Australian Fisheries
627 Management Authority and CSIRO Marine and Atmospheric Research, Hobart. 645 p.
- 628 Klaer, N. L. 2010. Tiger flathead (*Neoplatycephalus richardsoni*) stock assessment based on
629 data up to 2008. Pages 164-189 in Tuck G, N. (ed.) 2010. *Stock Assessment for the*

- 630 Southern and Eastern Scalefish and Shark Fishery 2009. Part 1. Australian Fisheries
631 Management Authority and CSIRO Marine and Atmospheric Research, Hobart. 334 p.
- 632 Klaer, N. L., S. E. Wayte, A. E. Punt, L. R. Little, A. D. M. Smith, R. B. Thomson, and G. N.
633 Tuck. 2009. Simulation testing of alternative Tier 3 assessment methods and control rules
634 for the SESSF. Pages 42-70 in Wayte, S.E. (ed.) 2009. Evaluation of New Harvest
635 Strategies for SESSF Species. CSIRO Marine and Atmospheric Research, Hobart and
636 Australian Fisheries Management Authority, Canberra. 137 p.
- 637 Little, L. R., and K. Rowling. 2009. Eastern Gemfish (*Rexea solandri*) stock assessment based
638 on 2008 survey data. Pages 167-208 in Tuck G, N. (ed.) 2009. Stock Assessment for the
639 Southern and Eastern Scalefish and Shark Fishery 2008. Part 1. Australian Fisheries
640 Management Authority and CSIRO Marine and Atmospheric Research, Hobart. 344 p.
- 641 Mace, P. M., and I. J. Doonan. 1988. A generalized bioeconomic simulation model for fish
642 population dynamics. New Zealand Fisheries Assessment Research Document 88/4,
643 MAFFish Fisheries Research Centre, Wellington.
- 644 MacCall, A. 2007. Appendix D - Depletion-adjusted average catch. Pages 27-30 in: Rosenberg,
645 A., D. Agnew, E. Babcock, A. Cooper, C. Mogensen, R. O'Boyle, J. Powers, G.
646 Stefansson, and J. Swasey, 2007. "Setting Annual Catch Limits for U.S. Fisheries: An
647 Expert Working Group Report". Lenfest Ocean Program, Washington DC. 36 p.
- 648 MacCall, A. 2009. Depletion-corrected average catch: a simple formula for estimating
649 sustainable yields in data-poor situations. ICES Journal of Marine Science, 66: 2267–
650 2271.
- 651 Methot, R. D. 2007. User Manual for the Integrated Analysis Program Stock Synthesis 2 (SS2).
652 Model Version 2.00b. 84 p.
- 653 Miller, T.J. and J.R. Skalski. 2006. Integrating design- and model-based inference to estimate
654 length and age composition in North Pacific longline catches. Canadian Journal of
655 Fisheries and Aquatic Sciences 63: 1092–1114.
- 656 Pauly, D. 1980. On the interrelationships between natural mortality, growth parameters, and
657 mean environmental temperature in 175 fish stocks. J. Cons. int. Explor. Mer 39: 175-
658 192.
- 659 Restrepo, V. R., and J. E. Powers. 1999. Precautionary control rules in US fisheries
660 management: specification and performance. ICES Journal of Marine Science 56: 846-
661 852.
- 662 Smith, A. D. M., K. J. Sainsbury, and R. A. Stevens. 1999. Implementing effective fisheries
663 management systems – management strategy evaluation and the Australian partnership
664 approach. ICES Journal of Marine Science 56: 967-979.

- 665 Smith, A. D. M., and D. C. Smith. 200 A harvest strategy framework for the SESSF. Report to
666 the Australian Fisheries Management Authority, Canberra, June 200
- 667 Smith, A. D. M., D. C. Smith, G. N. Tuck, N. Klaer, A. E. Punt, I. Knuckey, J. Prince, A.
668 Morison, R. Kloser, M. Haddon, S. Wayte, J. Day, G. Fay, F. Pribac, M. Fuller, B. Taylor,
669 and L. R. Little. 2008. Experience in implementing harvest strategies in Australia's south-
670 eastern fisheries. *Fisheries Research* 94: 373-379
- 671 Smith, A. D. M. and S. E. Wayte (eds). 2002. The South East Fishery 2001. Fishery Assessment
672 Report compiled by the South East Fishery Assessment Group. Australian Fisheries
673 Management Authority, Canberra.
- 674 Walters, C. J., and S. J. D. Martell. 2004. *Fisheries Ecology and Management*. Princeton
675 University Press. Princeton, USA.

Table 1 : Parameterisation of the operating model for the non-spatial scenarios. h is the steepness parameter of the spawner-recruit relationship, B_{curr}/B_0 is the spawning biomass relative to unfished prior to implementation of the HCRs, and n_A is the annual sample size for the age composition data.

#	Scenario	Type of selectivity curve	true M	h	B_{curr}/B_0	n_A	assumed M
1	base-case	asymptotic	0.08	0.75	0.40	100	0.08
2		asymptotic	0.08	0.75	0.20	100	0.08
3		asymptotic	0.08	0.75	0.75	100	0.08
4		asymptotic	0.12	0.75	0.40	100	0.12
5		asymptotic	0.12	0.75	0.20	100	0.12
6		asymptotic	0.12	0.75	0.75	100	0.12
7		asymptotic	0.18	0.75	0.40	100	0.18
8		asymptotic	0.18	0.75	0.20	100	0.18
9		asymptotic	0.18	0.75	0.75	100	0.18
10	low steepness	asymptotic	0.08	0.30	0.40	100	0.08
11		asymptotic	0.08	0.30	0.20	100	0.08
12		asymptotic	0.08	0.30	0.75	100	0.08
13	high steepness	asymptotic	0.08	1.00	0.40	100	0.08
14		asymptotic	0.08	1.00	0.20	100	0.08
15		asymptotic	0.08	1.00	0.75	100	0.08
16	dome-shaped selectivity	dome-shaped	0.08	0.75	0.40	100	0.08
17		dome-shaped	0.08	0.75	0.20	100	0.08
18		dome-shaped	0.08	0.75	0.75	100	0.08
19	assume wrong M	asymptotic	0.08	0.75	0.40	100	0.05
20		asymptotic	0.08	0.75	0.40	100	0.12
21		asymptotic	0.12	0.75	0.40	100	0.08
22		asymptotic	0.12	0.75	0.40	100	0.18

Table 2 : Parameterisation of the operating model for the spatial scenarios. ‘Full’ connectivity between regions implies single stock dynamics, ‘intermediate’ has 20% annual movement rate from one region to the other, while the ‘limited’ scenario only has a 5% annual movement rate. The movement patterns are as shown in Figure 1.

#	Scenario	Type of selectivity curve		true M	h	B_{curr}/B_0	n_A	assumed M	connectivity	movement pattern
		region 1	region 2							
1	base-case, full mixing	asymptotic	asymptotic	0.08	0.75	0.40	100	0.08	full	constant
2	intermediate mixing	asymptotic	asymptotic	0.08	0.75	0.40	100	0.08	intermediate	constant
3		asymptotic	asymptotic	0.08	0.75	0.20	100	0.08	intermediate	constant
4		asymptotic	asymptotic	0.08	0.75	0.75	100	0.08	intermediate	constant
5	limited connectivity	asymptotic	asymptotic	0.08	0.75	0.40	100	0.08	limited	constant
6		asymptotic	asymptotic	0.08	0.75	0.20	100	0.08	limited	constant
7		asymptotic	asymptotic	0.08	0.75	0.75	100	0.08	limited	constant
8	movement declines with age	asymptotic	asymptotic	0.08	0.75	0.40	100	0.08	intermediate	pre-recruit
9	movement increases with age	asymptotic	asymptotic	0.08	0.75	0.40	100	0.08	intermediate	adult
10	dome-shaped selectivity	dome-shaped	dome-shaped	0.08	0.75	0.40	100	0.08	intermediate	constant
11	differing selectivities	asymptotic	dome-shaped	0.08	0.75	0.40	100	0.08	intermediate	constant

Table 3 : Coefficients estimated from the linear models for the non-spatial analyses, by performance measure. Numbers shown represent terms that were assessed to be significant at the $\alpha = 0.05$ level in a full model that included all terms listed.

Linear predictor term	Performance measure						
	med(B_{final}/B_0)	IQR(B_{final}/B_0)	$P(B_{\text{final}} < B_{\text{lim}})$	$P(B_{\text{proj}} < B_{\text{lim}})$	med(avg TAC)	med(CV TAC)	# yrs collapse
base intercept (CR, old HCR, InitDepl=0.4, $h=0.75$, asymptotic Sel) MYEF		0.17	0.79	0.87	721	0.16	
new HCR, Ftarg=0.5M, Flim=M	0.14	0.10	-0.17	-0.13	-209	0.96	5.9
new HCR, Ftarg=F40, Flim=F20, adjust for h	0.17	0.15	-0.22	-0.15	-249	0.95	5.4
assumed $M >$ true M	-0.14	-0.26	0.35	0.22		0.54	4.6
assumed $M <$ true M	0.56		-0.64	-0.75	-468	0.85	5.7
Initial depletion = 0.75	0.39	0.24	-0.59	-0.64	476	0.20	
Initial depletion = 0.2				0.12	-394	0.62	4.8
$h = 1.0$	0.15		-0.17	-0.08			
$h = 0.3$	-0.14	-0.15	0.32	0.11		0.39	3.6
true $M = 0.12$					150		-1.3
true $M = 0.18$					1279		-2.4
new HCR, Ftarg=0.5M : Init Depl = 0.75 interaction	-0.58	-0.51	0.90	0.84	1108		
new HCR, Ftarg=F40 : Init Depl = 0.75 interaction	-0.60	-0.52	0.94	0.87			
new HCR, Ftarg=0.5M : Init Depl = 0.2 interaction	0.19		-0.32			-0.30	-2.8
new HCR, Ftarg=F40 : Init Depl = 0.2 interaction	0.23		-0.34				
dome-shaped selectivity : old HCR interaction							
dome-shaped selectivity : new HCR 0.5M interaction	0.12		-0.20	-0.14	-216		
dome-shaped selectivity : new HCR F40 interaction							

Table 4 : Values for the performance measures for the spatial analyses given estimation under MYEF, application of the new Tier 3 HCR, with $F_{TARG} = F_{40}$ and $F_{LIM} = F_{20}$. ‘ F option’ is the method used to obtain a single F_{CUR} estimate given the fleet and regional data (Section 3.3.3): 1) aggregate fleet and regional data, 2) obtain fleet and region-specific F estimates, weight by inverse variance, 3) separate analyses as in 2, but use the maximum estimated F to calculate the RBC. Scenario numbers as in Table 2.

F option	Scenario #	Performance measure						
		med(B_{final}/B_0)	IQR(B_{final}/B_0)	P($B_{final} < B_{lim}$)	P($B_{proj} < B_{lim}$)	med(avg TAC)	med(CV TAC)	# yrs collapse
1)	1	0.12	0.36	0.61	0.77	491	0.99	3.9
	2	0.24	0.35	0.42	0.69	479	0.95	2.6
	3	0.46	0.24	0.09	0.90	114	1.58	7.1
	4	0.00	0.00	0.97	0.98	1,944	1.48	5.3
	5	0.21	0.34	0.50	0.74	478	1.03	3.8
	6	0.47	0.22	0.07	0.86	90	1.56	7.2
	7	0.00	0.00	0.94	0.97	2,122	1.41	4.6
	8	0.21	0.42	0.47	0.58	458	1.02	4.1
	9	0.14	0.34	0.61	0.73	511	0.92	3.2
	10	0.47	0.44	0.26	0.33	288	1.00	2.6
	11	0.33	0.39	0.32	0.54	404	0.96	2.6
2)	1	0.15	0.42	0.55	0.72	436	1.04	4.1
	2	0.15	0.33	0.56	0.75	481	0.97	3.3
	3	0.44	0.22	0.09	0.87	109	1.53	6.8
	4	0.00	0.00	0.99	0.99	2,006	1.46	5.1
	5	0.19	0.42	0.56	0.71	479	1.05	3.7
	6	0.45	0.25	0.14	0.88	98	1.53	6.7
	7	0.00	0.00	0.97	0.97	2,161	1.47	5.2
	8	0.00	0.07	0.83	0.91	494	1.39	7.0
	9	0.07	0.36	0.60	0.73	508	0.92	3.3
	10	0.37	0.41	0.29	0.45	344	0.92	2.2
	11	0.22	0.40	0.46	0.60	443	0.94	2.9
3)	1	0.38	0.28	0.24	0.47	353	0.95	2.6
	2	0.35	0.36	0.26	0.48	367	0.98	2.9
	3	0.53	0.16	0.05	0.87	71	1.72	8.9
	4	0.00	0.11	0.83	0.84	1,899	1.27	3.5
	5	0.39	0.41	0.29	0.48	310	1.05	3.0
	6	0.52	0.18	0.02	0.83	46	1.86	10.2
	7	0.00	0.06	0.81	0.82	1,834	1.27	3.9
	8	0.62	0.23	0.01	0.07	135	1.12	3.5
	9	0.45	0.34	0.21	0.39	322	0.90	1.8
	10	0.59	0.27	0.12	0.22	205	1.02	2.9
	11	0.49	0.35	0.14	0.30	282	1.10	3.3

Table 5 : Coefficients estimated from the linear models for the spatial analyses. Numbers shown represent terms that were assessed to be significant ($p < 0.05$) in a full model that included all terms listed. Base intercept values were: *MYEF*, new HCR with $F_{TARG}=F40$ and $F_{LM}=F20$, obtain a single F estimate with all data, full mixing between regions, movement constant with age, initial depletion = 0.4, and $h=0.7$

Linear predictor term	Performance measure						
	med(B_{final}/B_0)	IQR(B_{final}/B_0)	P($B_{final} < B_{lim}$)	P($B_{proj} < B_{lim}$)	med(avg TAC)	med(CV TAC)	# yrs collapse
base intercept	0.19	0.37	0.51	0.71	468	0.97	3.5
wt regional F estimates by variance							
choose highest regional F	0.15		-0.21	-0.21	-141		
Initial depletion = 0.75	-0.25	-0.34	0.49	0.29	1562	0.39	1.4
Initial depletion = 0.2	0.22	-0.16	-0.36	0.23	-344	0.63	4.6
Different selectivities by region							
Selectivity dome-shaped in both regions	0.23		-0.21	-0.31	-145		
intermediate mixing							
limited mixing							
juveniles move only		-0.12				0.19	1.8
adults move only							

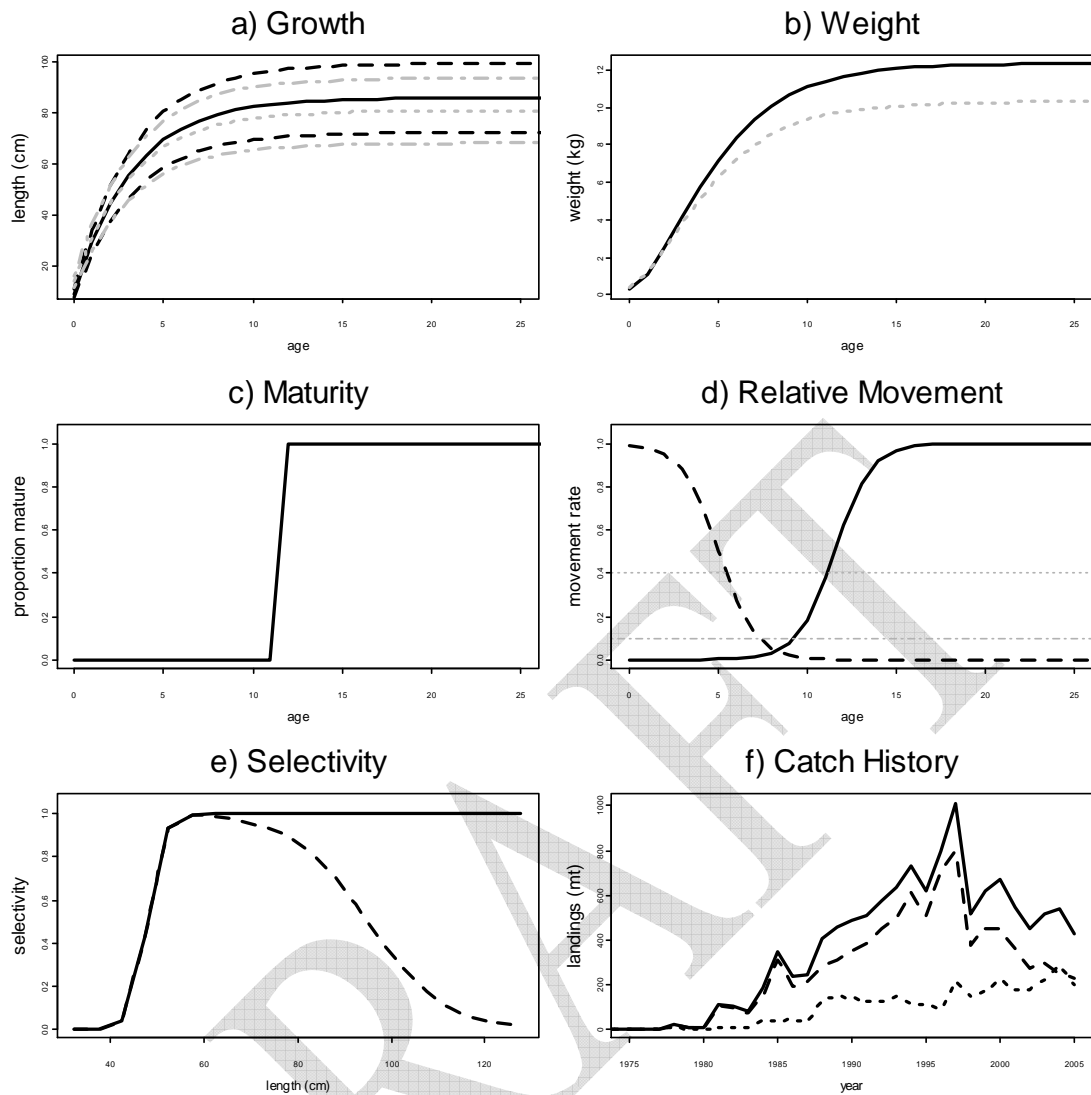


Figure 1 : Biological and fishery-related parameters. Top row of panels: values for females shown in black lines, males in grey. Solid lines in Growth panel represent mean lengths-at-age, dashed lines correspond to the 95% intervals of the distribution for length-at-age. Relative Movement panel shows pattern of relative movement rate for (solid) adult-only movement, and (dashed) pre-recruit movement. Gray dotted and dot-dashed lines indicate rates of movement (relative to “full” mixing scenario) for the “intermediate” and “limited” movement scenarios. Selectivity panel shows both asymptotic (solid line) and dome-shaped (dashed line) patterns with length. Catch history panel indicates both total catches (solid line) and regional catch histories used in the spatial analyses, with dashed line indicating catches from region 1, and dotted line indicating the catch from region 2.

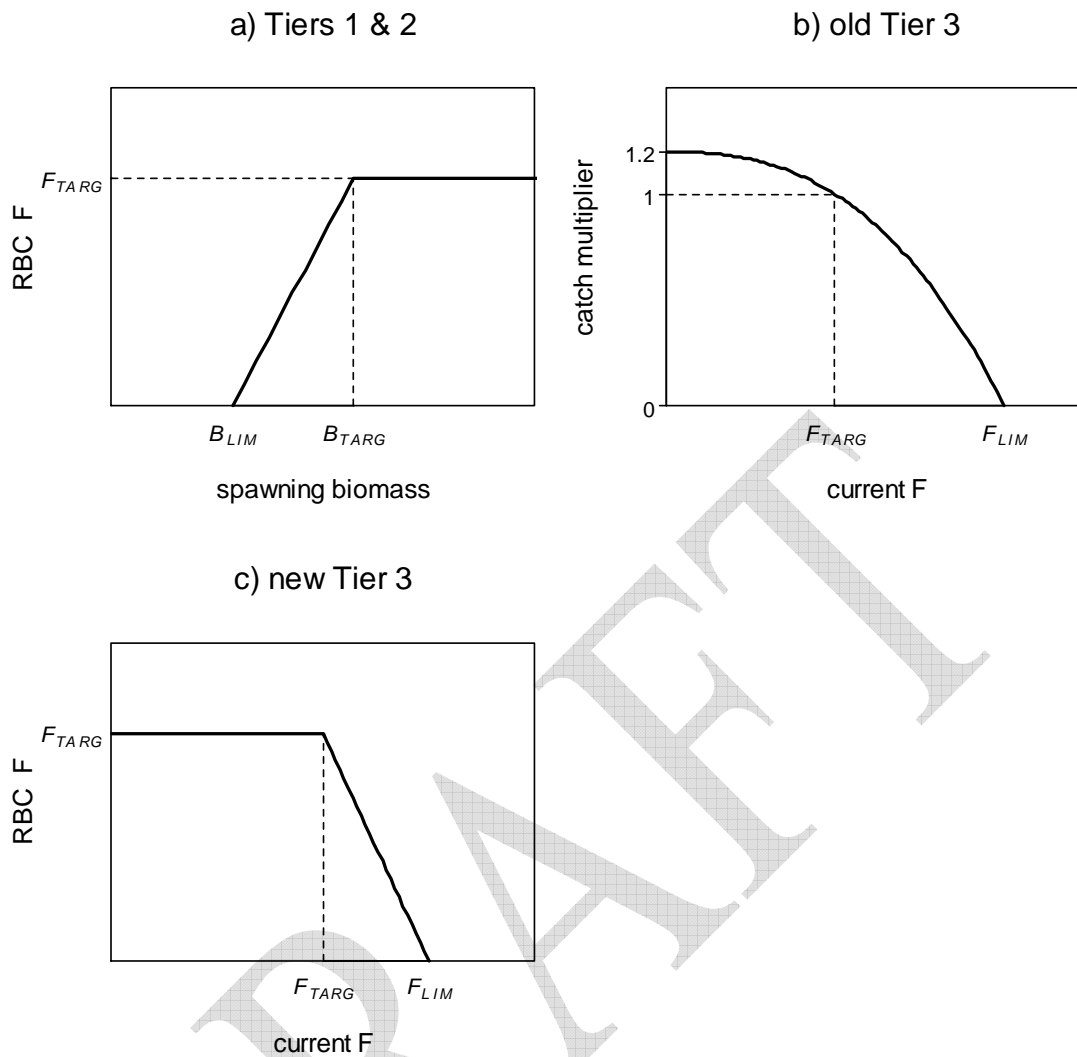


Figure 2 : Forms for the Harvest Control Rules (HCRs) for Tiers 1 and 2 (top-left panel), old Tier 3 (top-right panel), and new Tier 3 (bottom-left panel). The estimated value for the stock indicator on the x axis is used to derive either the RBC rate of fishing mortality (Tier 1 and new Tier 3), or the multiplier to the current catch (old Tier 3).

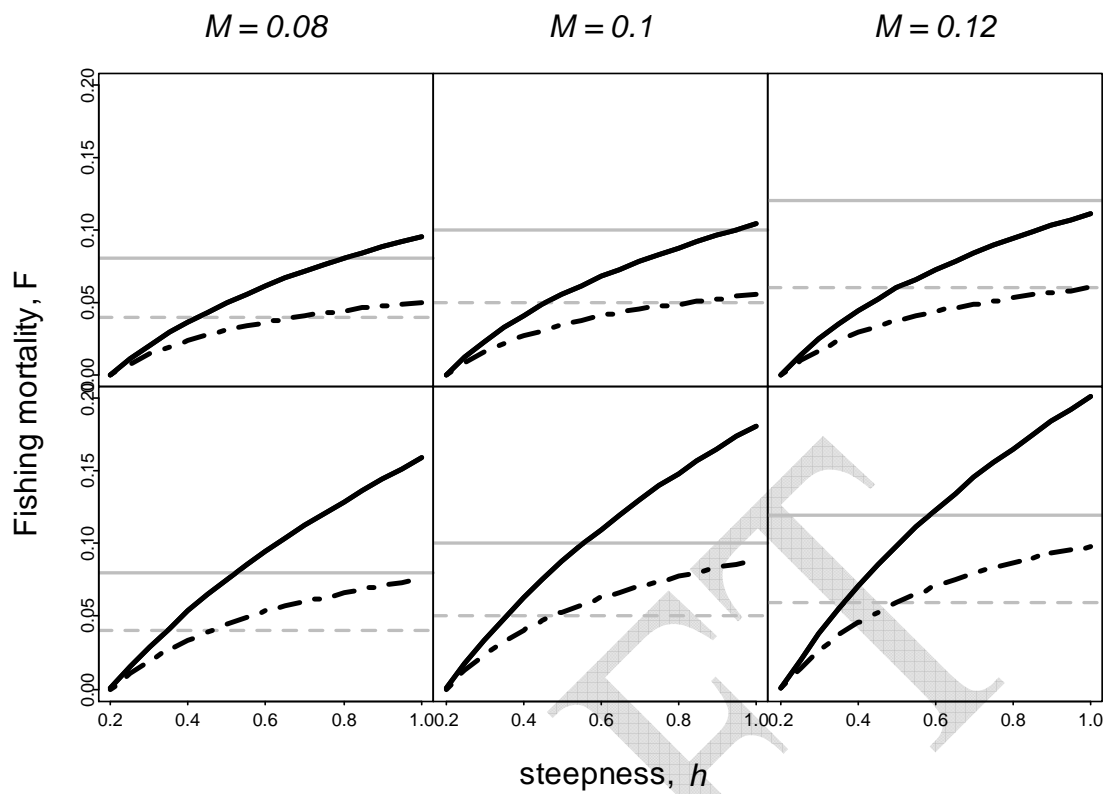


Figure 3 : Relationship between F_{40} (solid black line) and F_{20} (dot-dashed black line) and M , and h . The solid and dashed grey lines are M and $0.5M$ respectively. Top row of panels corresponds to an age-at-maturity of 12 yrs, as used in the analyses presented here. The bottom row of panels shows the change for an age-at-maturity of 6 yrs.

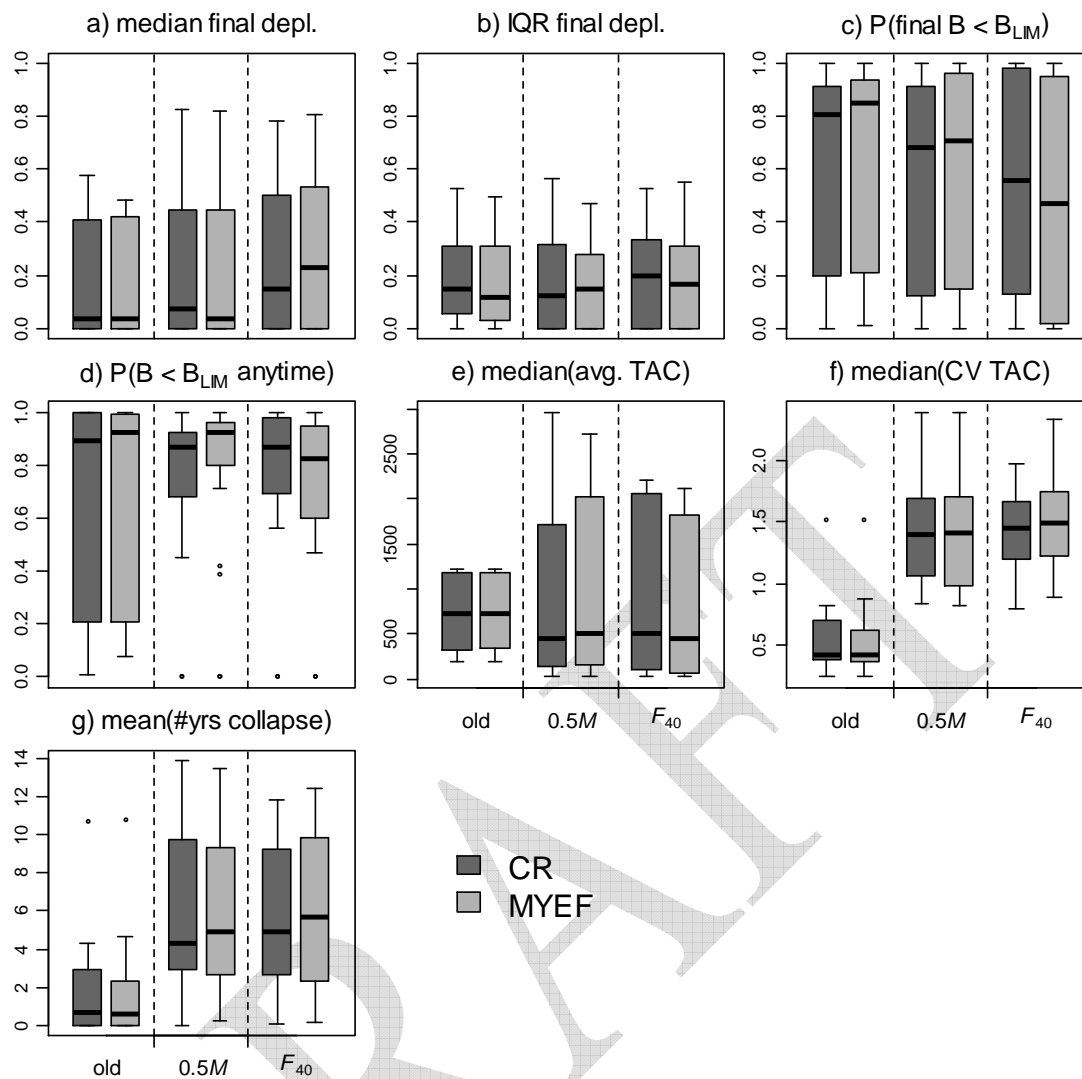


Figure 4 : Distribution of the performance measures across scenarios for the non-spatial analyses, for the two estimation methods, CR and MYEF, given application of the three HCRs (old = old Tier 3; $0.5M$ = new Tier 3 HCR with $F_{TARG} = 0.5M$. and $F_{LIM} = M$; F_{40} = new Tier 3 HCR with $F_{TARG} = F_{40}$ and $F_{LIM} = F_{20}$).

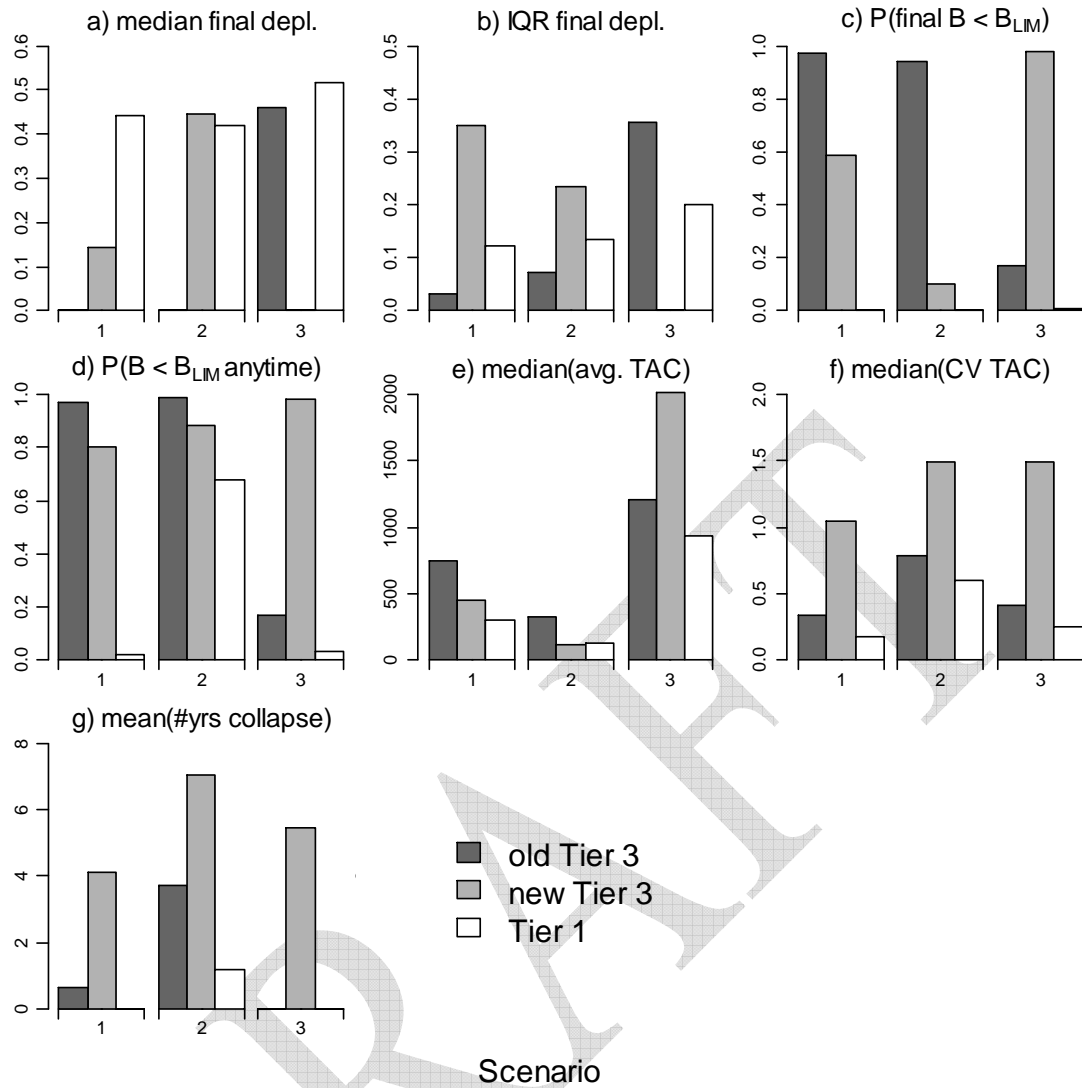


Figure 5 : Comparing performance of the old Tier 3 HCR, the new Tier 3 MYEF $F_{TARG} = F_{40}$, and the Tier 1 HCR, for three of the non-spatial scenarios. Numbers correspond to scenarios listed in Table 1.

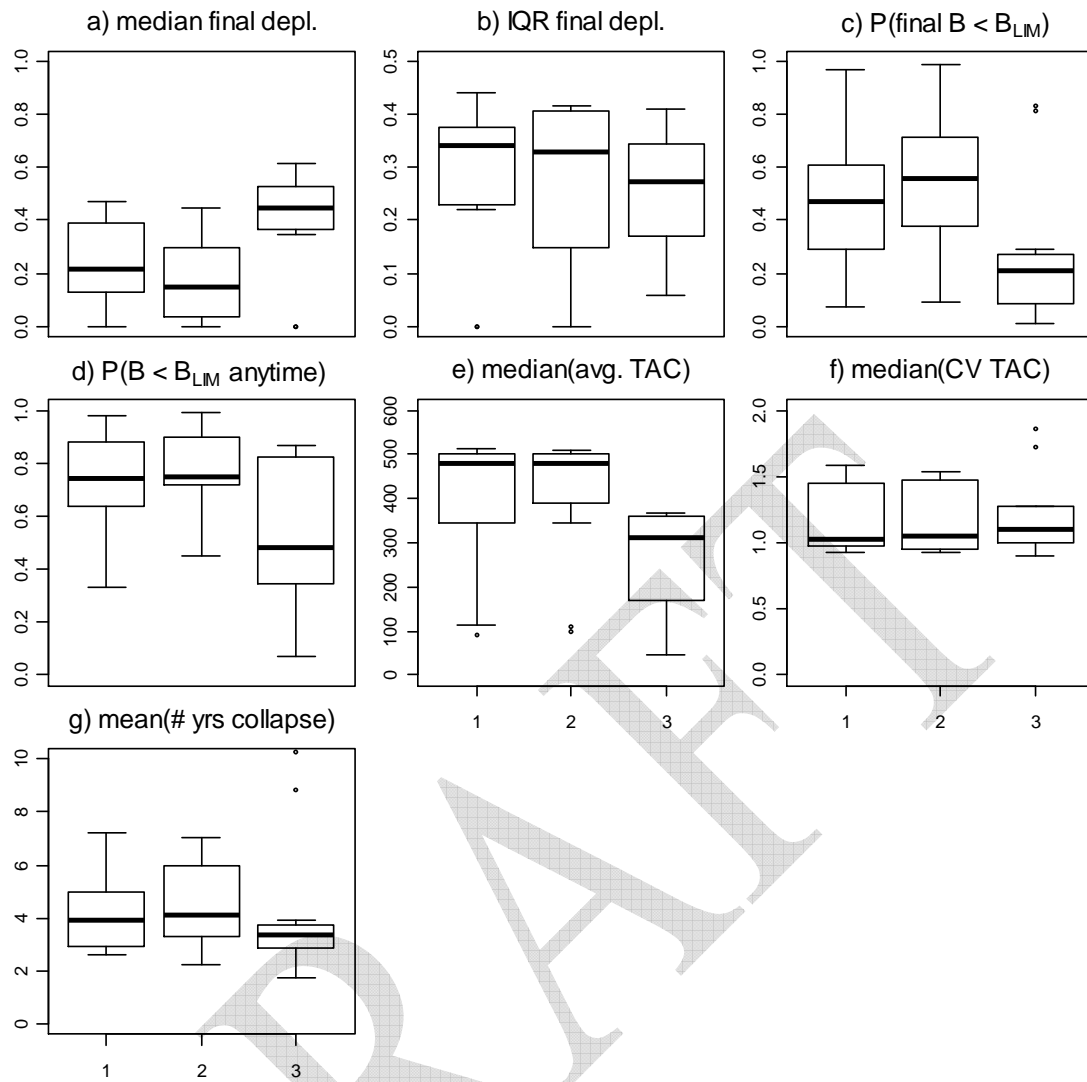


Figure 6 : Distribution of the performance measures across scenarios for the spatial analyses, for the different ways of choosing the annual F estimate (1 = aggregate data, 2 = analyse by region, weight estimates by variance, 3 = analyse by region and choose the maximum estimated F). Estimation is using MYEF with the new Tier 3 HCR with $F_{TARG} = F_{40}$ and $F_{LIM} = F_{20}$.

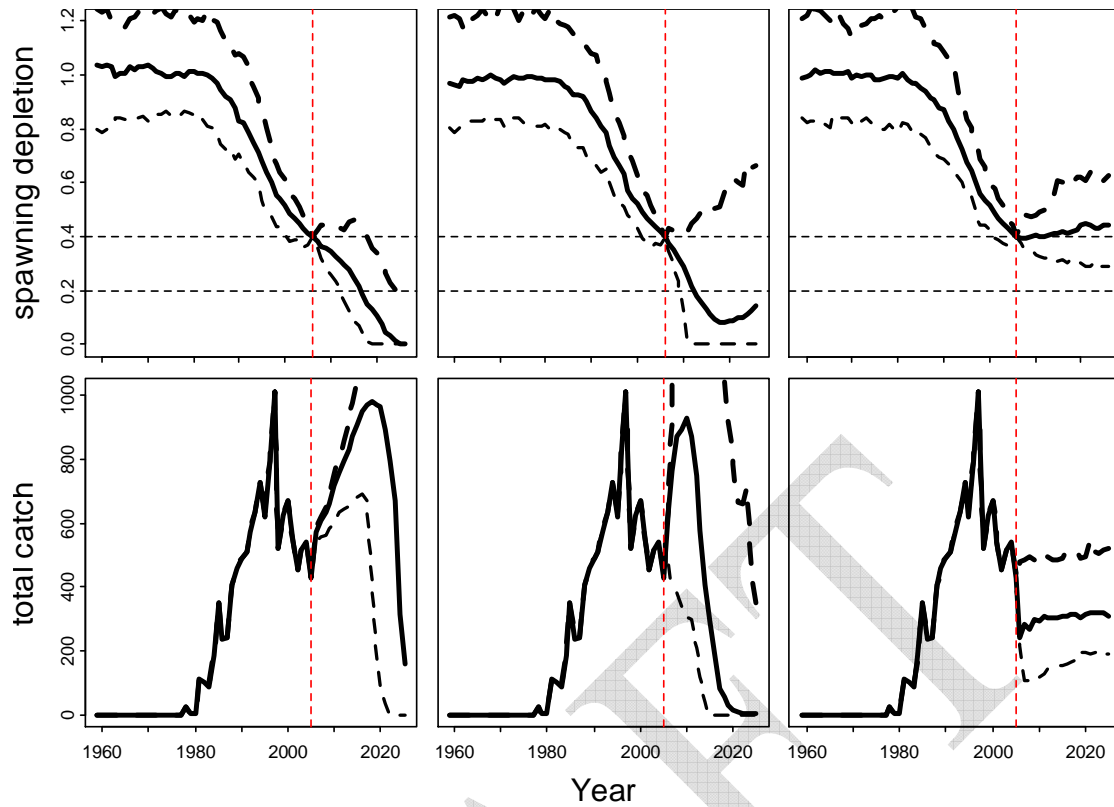


Figure 7 : Relative spawning biomass and catch trajectories for scenario 1 of the non-spatial analyses for (left) old Tier 3 HCR, (center) new Tier 3 HCR with MYEF and $F_{TARG}=F_{40}$, and (right) Tier 1. Plotted are the median (solid line) and central 95% interval (dashed lines) from the simulations. Red vertical line indicates the start of implementation of the harvest strategy, horizontal black dotted lines indicate the target (B_{40}) and limit (B_{20}) reference points.

1 Appendix 1. Operating Model Specifications

2 The operating model consists of an age-structured population dynamics model, a data-
3 generation module, and a component to allow future projections of the population model
4 given input from estimation methods and HCRs. The operating model can be appropriately
5 dimensioned and parameterised to account for several spatial regions and multiple fleets in
6 order to capture key dynamics for blue eye trevalla. The specifications are a simplified
7 version of those used to evaluate management strategies for a variety of species within the
8 SESSF (Fay et al. 2009).

9 A1.1 Population dynamics

10 The operating model includes one or more regions. Population dynamics operate at the level
11 of the fish stock, with a single stock occupying one or more regions. Fishing fleets operate in
12 one or more regions.

13 A1.1.1 Abundance dynamics

14 The number of animals of sex s and age a in region r at the start of year t , $N_{s,a,t}^r$ is given by:

$$15 \quad N_{s,a,t}^r = \begin{cases} \tilde{N}_{s,a-1,t-1}^r & \text{if } 1 \leq a < x \\ \tilde{N}_{s,x-1,t-1}^r + \tilde{N}_{s,x,t-1}^r & \text{otherwise} \end{cases} \quad (7)$$

16 where $\tilde{N}_{s,a,t}^r$ is the number of animals of sex s and age a in region r following mortality
17 (all sources) and movement during year t :

$$18 \quad \tilde{N}_{s,a,t}^r = \bar{N}_{s,a,t}^r + \sum_{r' \neq r} \bar{N}_{s,a,t}^{r'} X_{s,a}^{r',r} - \sum_{r' \neq r} \bar{N}_{s,a,t}^r X_{s,a}^{r,r'} \quad (8)$$

$$19 \quad \bar{N}_{s,a,t}^r = N_{s,a,t}^r e^{-M} (1 - u_{s,a,t}^r) \quad (9)$$

20 $X_{s,a}^{r',r}$ is the proportion of animals of sex s and age a moving from region r' to
21 region r ,

22 M is the rate of natural mortality,

23 $u_{s,a,t}^r$ the exploitation rate (due to all fleets) on animals of sex s and age a in region
24 r during year t :

$$25 \quad u_{s,a,t}^r = \sum_f \tilde{u}_t^{f,r} S_{s,a}^f \quad (10)$$

26 where:

$$\tilde{u}_t^{f,r} = \frac{C_t^{f,r}}{\sum_s \sum_L w_{L,s} S_L^f \sum_a \Phi_{L,s,a} N_{s,a,t}^r e^{-0.5M}} \quad (11)$$

27 $C_t^{f,r}$ is the retained catch by fleet f in region r during year t ,

28 $S_{L,t}^f$ is the selectivity of fleet f on animals in length bin L during year t ,

29 $\Phi_{L,s,a,t}$ is the proportion of fish of sex s and age a in length bin L during year t ,

30 $s_{s,a,t}^f$ is the selectivity of fleet f on animals of sex s and age a during year t ,

31 $w_{L,s}$ is the mean weight of a fish of sex s in length bin L , and

32 x is the maximum age (treated as a plus-group).

33 **A1.1.2 Selectivity**

34 The sex- and age-specific selectivity pattern for fleet f is calculated from the inputted length-
35 specific selectivity pattern:

$$36 \quad s_{s,a}^f = \sum_L S_L^f \Phi_{L,s,a} \quad (12)$$

$$37 \quad \Phi_{L,s,a} = \begin{cases} \tilde{\Phi} \left(\frac{l_L^{lo} - \bar{l}_{s,a}}{\sigma_{l_{s,a}}} \right) & \text{if } L=1 \\ \tilde{\Phi} \left(\frac{l_{L+1}^{lo} - \bar{l}_{s,a}}{\sigma_{l_{s,a}}} \right) - \tilde{\Phi} \left(\frac{l_L^{lo} - \bar{l}_{s,a}}{\sigma_{l_{s,a}}} \right) & \text{if } 1 < L < N_L \\ 1 - \tilde{\Phi} \left(\frac{l_L^{lo} - \bar{l}_{s,a}}{\sigma_{l_{s,a}}} \right) & \text{if } L = N_L \end{cases} \quad (13)$$

38 where $L = l_L^{lo} + 0.5 [l_L^{hi} - l_L^{lo}]$,

39 l_L^{hi} and l_L^{lo} are upper and lower limits of length bin L ,

40 $\tilde{\Phi}$ is the standard normal cumulative density function,

41 $\bar{l}_{s,a,t}$ is the mean length of a fish of sex s and age a in the middle of year t ,

42 $\sigma_{l_{s,a,t}}$ is the input standard deviation of the length of a fish of sex s and age a .

43 **A1.1.3 Growth**

44 The mean length-at-age by sex in year t is calculated by:

$$45 \quad \bar{l}_{s,a,t} = L_{\infty,s} \left(1 - \exp \left[k_s (a - t_{0,s}) \right] \right) \quad (14)$$

46 where $L_{\infty,s}$, k_s , and $t_{0,s}$ are the input growth parameters for animals of sex s .

47 Weight-at-length is governed by a length-power relationship:

$$48 \quad w_{L,s} = \alpha_s (L)^{\beta_s} \quad (15)$$

49 where α_s and β_s are the input parameters of the weight-length relationship for sex s .

50 **A1.1.4 Recruitment**

51 The annual recruitments (by region) are log-normally distributed about an underlying
52 Beverton-Holt stock-recruitment relationship (SRR):

$$53 \quad N_{s,0,t}^r = 0.5 R_t^r e^{\varepsilon_t^r - 0.5\sigma_R^2} \quad (16)$$

$$54 \quad R_t^r = \lambda_t^r \left(\frac{4hR_0 SB_t}{SB_0(1-h) + SB_t(5h-1)} \right) \quad (17)$$

55 where ε_t^r is the recruitment residual for region r and year t , which can be correlated
56 among regions:

$$57 \quad \boldsymbol{\varepsilon}_t \sim MVN(0, \boldsymbol{\Sigma}_t) \quad (18)$$

$$58 \quad \boldsymbol{\Sigma}_t = \sigma_R^2 \begin{pmatrix} 1 & \rho^{r_1 r_2} \\ \rho^{r_1 r_2} & 1 \end{pmatrix} \quad (19)$$

59 R_0 is the number of age-0 animals at pre-exploitation equilibrium,

60 h is the steepness of the stock-recruitment relationship,

61 SB_0 is the spawning biomass at pre-exploitation equilibrium (when recruitment
62 equals R_0),

63 σ_R is the standard deviation of the recruitment residuals,

64 $\rho^{r_1 r_2}$ is the correlation between the recruitment residuals for regions r_1 and r_2 , set to
65 1 (perfect correlation among regions) for this paper, and

66 λ_t^r is the expected fraction of the number of age-0 animals assigned to region r
67 during year t :

$$68 \quad \lambda_t^r = \tilde{S}B_t^r / SB_t \quad (20)$$

69 The total spawning biomass during year t is given by:

$$70 \quad SB_t = \sum_r \tilde{S}B_t^r = \sum_r \sum_{a=1}^x N_{\text{fem},a,t}^r \tilde{W}_{\text{fem},a} f_a \quad (21)$$

71 where f_a is the fraction of females of age a that are mature, and

72 $\tilde{w}_{\text{fem},a}$ is the weight at age of a female of age a at the start of the year:

73
$$\tilde{w}_{\text{fem},a} = \sum_L \Phi_{L,\text{fem},a} w_{L,\text{fem}} \quad (22)$$

74 **A1.1.5 Movement**

75 The probabilities of moving among regions are determined by:

76
$$X_{s,a}^{r',r} = \frac{\bar{X}_{s,a}^{r',r}}{\sum_{r'} \bar{X}_{s,a}^{r',r}} \quad (23)$$

77 where $\bar{X}_{s,a}^{r',r}$ is the average probability of an animal of sex s and age a moving from region
78 r' to region r :

79
$$\bar{X}_{s,a}^{r',r} = \begin{cases} T_s^{r',r} m_{s,a} & \text{if } r' \neq r \\ 1 - \sum_{r' \neq r} T_s^{r',r} m_{s,a} & \text{otherwise} \end{cases} \quad (24)$$

80 $T_s^{r',r}$ is the maximum average probability of moving from region r' to region r ,
81 with $T_s^{r',r} = 1$, and

82 $m_{s,a}$ is the relative age-specific movement rate for an animal of sex s .

83 **A1.1.6 Initial Conditions**

84 The initial ($t=1$) numbers at age for each sex by region are determined by solving the
85 following set of linear equations:

86
$$\mathbf{N}_{s,1} = (\mathbf{I} - \mathbf{G}_s)^{-1} \tilde{\mathbf{R}}_{s,1} \quad (25)$$

87 where $\mathbf{N}_{s,1}$ is an $(x+1) \times N_{\text{reg}}$ (number of regions) vector containing the initial age-
88 structure for animals of sex s ,

89 $\tilde{\mathbf{R}}_{s,1}$ is the corresponding vector of recruits with elements:

90
$$\tilde{R}_{s,a,1}^r = \begin{cases} 0.5 \lambda_0^r R_0 & \text{if } a = 0 \\ 0 & \text{if } 1 \leq a \leq x \end{cases} \quad (26)$$

91 where λ_0^r is the fraction of recruits allocated to region r in equilibrium, the value for
92 which is solved for in order to satisfy equation (20), and

93 \mathbf{G}_s is a square transition matrix with the same dimension as $\mathbf{N}_{s,1}$, describing the
94 mortality and movement pattern, the elements of which are obtained from the
95 equations for the population update:

$$96 \quad G_{s,a_p,a_q}^{r_p,r_q} = \begin{cases} X_{s,a_p}^{r_q,r_p} e^{-M} & \text{if } a_p = a_q - 1 \\ X_{s,a_p}^{r_q,r_p} e^{-M} & \text{if } a_p = a_q = x \\ 0 & \text{otherwise} \end{cases} \quad (27)$$

97 a_p is the age associated with row p ,

98 a_q is the age associated with column q ,

99 r_p is the region associated with row p , and

100 r_q is the region associated with column q .

101 **A1.2 Generating Age-composition Data**

102 The observed catch-at-age proportions by region, sex and fleet are a multinomial sample of
 103 size $n_{s,t}^{f,r}$ from the true catch-at-age proportions. The proportion of the catch that is of age a
 104 during year t for fleet f and sex s in region r is:

$$105 \quad p_{a,s,t}^{f,r} = \frac{\tilde{C}_{s,a,t}^{f,r}}{\sum_a \tilde{C}_{s,a,t}^{f,r}} \quad (28)$$

106 where:

$$107 \quad \tilde{C}_{s,a,t}^{f,r} = I^{f,r} \sum_L S_L^f \Phi_{L,s,a} N_{s,a,t}^r e^{-0.5M} \quad (29)$$

108 $I^{f,r}$ is an indicator equal to 1 if fleet f operates in region r , and zero otherwise.

109 The individual $n_{s,t}^{f,r}$'s by fleet and region are derived from a multinomial sample of the total
 110 annual age-composition with relative probability given by $C_t^{f,r}$ and sample size 100. As
 111 such, the ageing samples are (on average) proportionally allocated by fleet and region with
 112 respect to the annual catch.

113 **A1.3 Allocation of TAC by fleet and region during projection** 114 **period**

115 For each year of the projection period, the catches for each fleet and region are calculated
 116 using a multinomial allocation of the total TAC for that year. The expected proportions of the
 117 catch for each fleet/region are:

$$\begin{aligned}
 118 \quad p_{C,t}^{f,r} &= \frac{C_t^{f,r}}{\sum_{f'} \sum_{r'} C_t^{f',r'}} = \frac{\tilde{p}_{C,t}^{f,r}}{\sum_{f'} \sum_{r'} \tilde{p}_{C,t}^{f',r'}} \\
 \tilde{p}_{C,t}^{f,r} &= \frac{\xi^{f,r} + \psi^{f,r} (B_t^{f,r})^{\zeta^{f,r}}}{\sum_{f'} \sum_{r'} \left[\xi^{f',r'} + \psi^{f',r'} (B_t^{f',r'})^{\zeta^{f',r'}} \right]} \quad (30)
 \end{aligned}$$

119 where $\xi^{f,r}$, $\psi^{f,r}$, and $\zeta^{f,r}$ are the parameters of the relationship between biomass
 120 distribution and catch allocation, and

121 $B_t^{f,r}$ is the vulnerable biomass in region r for fleet f in the middle of year t :

$$122 \quad B_t^{f,r} = I^{f,r} \sum_s \sum_L w_{L,s} S_L^f \sum_a \Phi_{L,s,a} N_{s,a,t}^r e^{-0.5M} \quad (31)$$

123 The values of the parameters $\xi^{f,r}$, $\psi^{f,r}$, and $\zeta^{f,r}$ are determined by fitting the multinomial
 124 model in equation (30) to the (known) historical catch proportions by fleet and region.

125 **A1.4 References**

126 Fay, G., A. E. Punt, and A. D. M. Smith. 2009. Operating model specifications. Pages 125-
 127 133 in Wayte, S.E. (ed.) 2009. Evaluation of New Harvest Strategies for SESSF
 128 Species. CSIRO Marine and Atmospheric Research, Hobart and Australian Fisheries
 129 Management Authority, Canberra. 137 p.